Carbonates Evaporites (2010) 25:231–246
DOI 10.1007/s13146-010-0028-z

Petrographical and geochemical evidences for paragenetic sequence interpretation of diagenesis in mixed siliciclastic–carbonate sediments: Mozduran Formation (Upper Jurassic), south of Agh-Darband, NE Iran

A. Mahboubi · R. Moussavi-Harami ·
S. J. Carpenter · A. Aghaei · L. B. Collins

Accepted: 29 June 2010

Petrographical and geochemical evidences for paragenetic sequence interpretation of diagenesis in mixed siliciclastic–carbonate sediments: Mozduran Formation (Upper Jurassic), south of Agh-Darband, NE Iran

Mahboubi, A.[1*], Moussavi-Harami, R.[1], Carpenter, S.[2], Aghaei A.[1] and Collins[3], L.B.

1. Department of Geology, Faculty of Science, Ferdowsi University of Mashhad, 91775-1436, Iran
2. Department of Geology, University of Iowa, USA
3. Department of Applied Geology, Curtin University of Technology, Perth, Western Australia

Abstract

The Upper Jurassic Mozduran Formation with thickness 420 meters at the type locality is the most important gas-bearing reservoir in NE Iran. It is mainly composed of limestone, dolostone with shale and gypsum interbeds that grade into coarser siliciclastics in the easternmost part of the basin. Eight stratigraphic sections were studied in detail in south of the Agh-Darband area. These analyses suggest that four carbonate facies associations and three siliciclastic lithofacies were deposited in shallow marine to shoreline environments, respectively. Cementation, compaction, dissolution, micritization, neomorphism, hematitization, dolomitization and fracturing are diagenetic processes that affected these sediments. Stable isotope variations of $\delta^{18}O$ and $\delta^{13}C$ in carbonate rocks show two different trends. High depletion of $\delta^{18}O$ and low variation of $\delta^{13}C$ probably reflects increasing temperatures during burial diagenesis, while the higher depletion in carbon isotope values with low variations in oxygen isotopes are related to fresh water flushing during meteoric diagenesis. Negative values of carbon isotopes may have also resulted from organic matter alteration during penetration of meteoric water. Fe and Mn enrichment with depletion of $\delta^{18}O$ also supports the contention that alteration associated with higher depletion in carbon isotope values with low variations in oxygen isotopes took place during meteoric diagenesis. The presence of bright luminescence indicates redox conditions during precipitation of calcite cement.

Keywords: Jurassic, Diagenesis, Carbonate, Iran, Kopet-Dagh Basin

1* Corresponding author email address: amahboobi2001@yahoo.com and mahboubi@ferdowsi.um.ac.ir.
Fax number: 0098 511 8797275

Introduction

The Kopet-Dagh petroliferous basin of northeast Iran and southwest Turkmenistan formed after closure of the Hercynian Ocean following the Middle Triassic Orogeny (Berberian and King 1981; Ruttner 1993; Alavi et al. 1997). More than 7000 meters of carbonate, siliciclastic and evaporite sediments were deposited from Jurassic through Miocene time in the eastern parts of the basin (Afshar-Harb 1979, 1994) that formed five major transgressive-regressive sequences (Moussavi-Harami and Brenner 1992). The major reservoir in the giant Khangiran gas field in the Kopet-Dagh basin is a highly porous and permeable dolomitic interval of the Upper Jurassic (Oxfordian–Kimmeridgian) Mozduran Formation. This formation at type locality is mainly composed of limestone, dolostone and lesser amounts of shale interbeds; ranging in thickness from 420 to 1380 meters at the type section and Khangiran well #31 respectively (Afshar-Harb 1994). These carbonate rocks grade laterally to coarser siliciclastic and evaporite sediments in the Agh-Darband area in the easternmost parts of the basin (Moussavi–Harami 1989). The Mozduran Formation disconformably overlies marine shale of the Kashafrud Formation and is underlain by red siliciclastic rocks of the Shurijeh Formation that have been deposited by fluvial depositional systems.

The objectives of this study are recognition of diagenetic processes and interpretation of their paragenetic sequences operated on the Mozduran Formation during post Oxfordian–Kimmeridgian time.

Methods and material studied

In this study eight stratigraphic sections from the Mozduran Formation (ranging in thickness from 89 to 509 meters) south of the Agh-Darband area (Fig.1) were measured. 750 thin sections were etched with dilute HCl and stained with Alizarin Red and Potassium Ferricyanide solution based on Dickson (1966) for differentiation of calcites and dolomites (ferroan and non-ferroan) and 120 washed samples were studied by polarized and binocular microscopes respectively. In addition, 150 polished thin sections were studied with a cathodoluminescence microscope (Marshall 1988; Tucker 1988, Frank et al. 1995), using a Technosyn Cold CL (Model 8200 MK3) at 12 KV and 195 µA with an automatic camera.

Thirty limestone samples were analyzed for carbon and oxygen isotopes as well as trace elements. A microscope-mounted dental drill was used to extract calcite powder from polished specimens. About 0.2 mg of each sample was reacted with anhydrous phosphoric acid in individual reaction vessels in a vacuum at 72°C. The CO_2 extracted from each sample was analyzed by isotope ratio mass spectrometry at the Nelson Laboratory at the University of Iowa. Both $\delta^{18}O$ and $\delta^{13}C$ values are reported relative to PDB. The same sample powders

were also analyzed by Atomic Absorption Spectrophotometer to determine their Ca, Mg, Sr, Na and Fe content at the geochemistry laboratory at the Ferdowsi University of Mashhad.

Fig.1

Depositional environments

The Upper Jurassic Mozduran Formation in the study area is composed of both carbonate and siliciclastic rocks. Based on petrographical studies, four carbonate facies associations (A to D), three major siliciclastic (G and F) and one evaporate lithofacies (E) have been identified (Mahboubi et al. 2006) (Table 1 and Fig. 2).

Facies association A consists of echinoderm brachiopod packstone and brachiopod red algal grainstone, association B is composed of ooid bearing pelecypod grainstone, ooid grainstone, ooid bioclast intraclast grainstone, association C is also mainly composed of ooid-bioclast packstone, green algal wackestone, coral fragments wackestone, lime mudstone, peloidal packstone and peloidal grainstone and finally association D consists of dolomudstone and lime mudstone. Siliciclastic lithofacies consist of sandstones (F) including quartzarenite, sublitharenite, litharenite and fossiliferous litharenite, gypsiferous shales (G).

Table 1

The presence of many stenohaline organisms, such as echinoderms and brachiopods of medium-to-fine sand-size in association A indicates possible open marine conditions below the fair-weather wave base (e.g. Sanders and Hofling 2000; Flugel 2004; Schneider et al. 2004). Seemingly, oolitic cross-bedded grainstones of association B, were deposited in higher energy environments, such as barriers (e.g. Martin-Chivelet et al. 1995; Alsharhan and Kendall 2003; Coffey and Read 2004). Presence of pelloids within the mud-supported and medium-to-thin-bedded packstones indicate a low energy lagoonal environment for association C (e.g. Burchet et al. 1990; Alsharhan and Kendall 2003; Adachi et al. 2004). Thin-bedded dolomudstone and lime mudstone with gypsum interbeds suggest deposition of association D in a supra-tidal environment (e.g. Yechieli and Wood 2003; Alsharhan and Kendall 2003; Fortuin and Krijgman 2003; Warren 2006).

Mature-to-super mature litharenite to sublitharenite with trough and herringbone planar cross-lamination and cross-bedding as well as coarsening and thickening upward cycles of sandstones to pebbly sandstone in

easternmost part (Figs. 2 and 3) show that these sediments may have been deposited in a high energy tidal dominated shoreline (based on Miall 1997; Tamura and Masuda 2003 and Holz 2003 in other places). Fine grained mudrocks with evaporate minerals also show low-energy restricted conditions.

Based on the combination of field observations, laboratory considerations, as well as vertical and lateral facies changes in the studied area, it is interpreted that the carbonate facies were deposited on a homoclinal carbonate ramp in open marine, barrier, lagoon and tidal flat sub environments, whereas siliciclastic lithofacies were deposited during times of high siliciclastic influx in tidal environments (Fig. 3).

Fig. 2

Fig. 3

Diagenetic events

Diagenetic processes that affected these various rock types during short as well as long periods after deposition will be explained and interpreted separately for carbonate and coarser siliciclastics.

Diagenetic features in limestones

Petrographic studies showed that several diagenetic processes including micritization, compaction, cementation, neomorphism, dissolution, dolomitization, fracturing and vein formation have affected limestones of the Mozduran Formation.

Micritization: Micritization is the first diagenetic process that occurs at the sediment-water interface (Adams and Mackenzie 1998) under low energy conditions (Tucker and Wright 1990; Flugel 2004). This process is generated by repetition of microorganism activities by bacteria, algae and fungi on carbonate grain surfaces (Carols 2002). Micritization in studied samples affected many skeletal grains such as plecypod and brachiopod as well as non-skeletal particles such as ooid and intraclasts (Fig. 4A). It formed thin micrite envelopes with around some grains and in others this process led to destruction of most parts with patches of micrite present.

Cementation: Cement fabrics formed in various diagenetic environments are:

a) Isopachous fringing cement: This formed as the first generation cement around ooids and bioclasts in grainstones. It shows fibrous and bladed shapes and formed on the grain rims or micrite envelops (Fig. 4B.a). Isopachous cements reflected high saturation state of $CaCO_3$ and low sedimentation rate during its formation (Ehrenberg et al. 2002).

b) Blocky cement: This formed in mud-free grain-supported lithofacies comprising single crystals with 0.1 to 0.25 mm in diameter. This cement is the second generation cement which generally occupies remains of pore space after isopachous fringing cements (Fig. 4C). Blocky cements have a blue color with potassium ferricyanide solution that shows presence of Fe. This cement has also alternatively dark, bright and dull luminescence zones under CL microscope indicating the presence of various amounts of Fe and Mn content during precipitation (Fig. 6A and B).

c) Mosaic cement: This is less common cement and formed as subhedral crystals with average size ranging from 0.05 to 0.1 mm. that filled pores between skeletal and non-skeletal grains (Fig. 4B.b).

d) Poikilotopic cement: This cement type consists of a large crystal that contains several smaller bioclast grains (Fig. 4D). It is not common in studied samples and it may have been deposited from supersaturated pore fluids of calcium carbonate with low nucleation rate of calcite crystals and low growth rate. This condition can be present during burial diagenesis (Flugel 2004).

e) Syntaxial overgrowth rim cement: This cement is formed in bioclastic grainstones around the echinoderm fragments. It is generally clear and lacking inclusions (Fig. 4E).

Compaction: Compaction affected limestones of the Mozduran Formation after deposition and led to physical and chemical rearrangements and changes in the sediments. Close packing, close grain contacts and decreasing of primary interparticle porosity in grain supported-limestones support physical compaction. Evidently, physical compaction may have more affected shale interbeds within the limestone units and led to dewatering and decreasing of thickness. As overburden increased and sediments buried deeply, chemical compaction started and changed some of the sediment characteristics (Fig. 4F and G). Evidence includes closer packing, increasing suture and concave-convex contacts, fracturing ooid and some shells such as brachiopods, bryozoans and echinoderms, pressure dissolution at grain contacts and the formation of stylolites (e.g. Vincent et al. 2007).

Fig. 4

Dissolution: This process has affected most of the carbonate rocks in the study area. Penetration of undersaturated water led to dissolution of grain and matrix in many limestones. Generation of secondary porosity was the most important result of this event. This type of porosity in many samples is non-fabric selective, although selective dissolution has also occurred (Fig. 5A). This later type was mainly formed during

exposure of limestones. Oomoldic porosity is another manifestation of dissolution that is mainly seen in ooid grainstones. In addition, some meta-stable and unstable grains such as aragonitic bioclasts were dissolved during deep burial and chemical compaction. This evidence is well seen in close packed grain-supported facies.

Neomorphism: Neomorphism occurs in presence of water during dissolution and precipitation (Bathurst 1975; Tucker 1993). Two types of neomorphism are observed in studied samples. a) Transfer and change of lime mud to coarser crystals in mud-supported facies and b) filling of some shells with sparry calcite such as pelecypods and gastropods that formed from metastable aragonite mineralogy. The last type is mainly seen in bioclastic grainstone and packstone in the studied samples (Fig. 5B).

Dolomitization: One of the most important processes that affected many limestones in the study area is dolomitization. Based on petrographic evidence (e.g., Sibely and Greeg classification 1987), dolomites in the study area have been divided into three types: Type one ($D_{1)}$ is a fine crystal with anhedral to subhedral shape and the size is less than 100 micron (Fig. 5F). These dolomites are associated with evaporite minerals such as gypsum. Type two (D_2) is medium crystal size (100 to 300 micron) and subhedral to planar euhedral. This type of dolomite is mostly observed as a replacement in limestone and cement within sandstones. Replacement is often observed as fabric-destructive in some carbonate grains of grainstones such as echinoderms, pelecypods, intraclasts and rarely ooids (Fig. 5G). Dolomites type three (D_3) have coarse crystal size (more than 300 micron) and are planar euhedral to subhedral. These crystals mainly fill pores and fractures (Fig. 5H). These dolomites have cloudy centers and clear rims. Kyser et al. (2002) interpreted that these dolomites can be generated from different fluids. Different crystal size in three types of dolomites (D_1, D_2 and D_3) can be accounted for by the relationship between nucleation and kinetic growth as well as relative timing. In fine crystalline dolomites, nucleation rate is higher than crystal growth rate and in coarse crystalline types crystal growth rate is higher than nucleation rate. Both nucleation and crystal growth rates increase with temperature (Sibely and Greeg 1987).

Fractures and Veins: Veins in the studied carbonate rocks are abundant. These veins have been filled with coarse crystalline sparry calcite (Fig. 5C). Cathodoluminscence study indicates that several dark-bright luminescence zones in these samples can be related to fluctuation of chemical composition of fluids during calcite precipitation (Fig. 6B) (Marshall 1988; Fouke et al. 2002).

Diagenetic features in sandstones

Sandstone affected by compaction, cementation, dissolution, dolomitization, and fracturing and vein formation during deposition and post deposition time.

Compaction: compaction of sandstones led to physical change in grain packing and orientation. Sediment loading and tectonic subsidence from the Jurassic through Neogene (Moussavi-Harami and Brenner 1992) and later orogenic events in this basin were the main causes of compaction that affected the sandstones. Early cementation was one of the most important factors that helped reduce compaction effects in sandstones (e.g. Kim and Lee 2004). High cement/grain ratio and loose packing are the common features in some sandstone that indicate that cementation operated during the early stages of diagenesis. In some samples with no early cement, closer packing, high grain/cement ratio, high linear, sutured and concave-convex contacts are the most common evidence for operation of compaction at the early stage before the effect of cementation in the studied samples.

Cementation: Carbonate (calcite and dolomite) and silica are the most common cement types in these sandstones (Fig. 5D and E). Calcite cement is mainly fine crystals with granular fabric but in some samples it is in blocky form. Petrographic studies suggest that calcite may have had two sources. First, pressure dissolution of bioclastic grains between terrigenous particles during burial compaction (mesogenesis) and secondly comes from fluid derived during burial compaction of limestone interbeds. Silica cement is less common than carbonate and is mostly seen as an overgrowth around the quartz grains. This implies that silica cement precipitated in favorable sites where enough pore space was available. Sediments may retain this type of pore space during early stages of burial (Ahmad and Bhat 2006). Silica could have been derived from different sources. In studied samples, dissolution of quartz grains at their boundaries, feldspar alteration and diagenesis of clay minerals, saturated fluids from silica, are the most important sources for quartz cementation (e.g. Ahmad and Bhat 2006)

Dissolution: Dissolution of carbonate cements is one of the most important factors that increased secondary porosity in the sandstones studied. This process may have taken place during the late burial diagenetic stage when the acidic waters formed from carboxylation generated from organic matter in shales moved into these coarser-grain sediments (e.g. Ahmad and Bhat 2006; Machent et al. 2007).

Dolomitization: Dolomitization is abundant in many types of sandstone**,** and based on the above classification (described in limestone diagenesis) they are mostly of D_2 and D_3 types with small amounts of D_1 type.

Hematitization: Hematite is present in many samples as cement, especially around grains. The source of iron could be from diagenesis of clay minerals, or may have come into the depositional site by meteoric waters.

Hematite shows evidence for dominantly oxidizing conditions during deposition of sandstones (Weible and Friis 2004). Therefore, we believe that the main source of iron was from meteoric water. Also the presence of opaque mineral grains including limonite and hematite suggests derivation from metamorphic and igneous rocks (e.g. Ahmad and Bhat 2006).

Fig. 5

Fig. 6

Stable Isotope geochemistry

Results: To establish a better understanding of diagenetic processes that operated after deposition of the Upper Jurassic limestones in the study area, 30 samples were analyzed for carbon and oxygen isotopes. These analyses have been done on grains such as ooids, brachiopods as well as cement and lime mud (Table 2).

Table 2

Discussion: Cross plots of carbon versus oxygen isotope values have been used by many researchers for geochemical interpretation (e.g. Hudson 1977; Anderson and Arthur 1983; Lohmann 1988; Morse and Mackenzie 1990; Nelson and Smith 1996; Rahimpour-Bonab et al. 1997; Macaulay et al. 2001; Mahboubi et al. 2004, 2006; Adabi et al. 2006). Data cross plots of the Upper Jurassic limestones (Fig. 7) show two different trends. First, a trend with low changes in $\delta^{13}C$ values and higher variation in $\delta^{18}O$, and second a higher variation in $\delta^{13}C$ values and low change in $\delta^{18}O$ values. These variations are obviously related to abundance of fluid types during sediment deposition. In general, open systems and high water-rock ratio lead to loss of primary isotopic values, while closed systems and low water-rock ratios favor presentation or total retention of original isotopic composition (Meyers 1989). The first trend with high depletion of $\delta^{18}O$ probably reflects increasing temperature during burial diagenesis which is similar to what Choquette and James (1987) and Nelson and Smith (1996) have described. Low variation in $\delta^{13}C$ values could have resulted from original inorganic carbon derived as well

as less differentiation between $^{13}C/^{12}C$ ratios than $^{18}O/^{16}O$ ratios with increasing temperature. The second trend that shows higher depletion in carbon isotope value is relatively similar to the inverted J trend of Lohmann (1988) and is usually supported by flushing of fresh water during meteoric diagenesis. Negative values of carbon isotopes could have resulted from organic matter alteration during penetration of meteoric water. The Lower Cretaceous unconformity could have also allowed meteoric water recharges in the Lower and Upper Jurassic formations and increased the effect of meteoric water on these deposits (e.g. Vincent et al. 2007).

Fig. 7

Comparison of these data with others (Milliman and Muller 1977, James and Choquette 1983 and Adabi and Rao 1991) (Fig. 7) shows greater depletion of oxygen isotope values due to intensive diagenetic effects. In addition, comparison of these data with previous isotopic data from the Mozduran Formation to the north in the Kopet-Dagh Basin (Adabi and Rao 1991) shows the same results. This trend shows that important effects of meteoric and burial diagenesis on the oxygen isotopic composition causing depleted. However, it is also possible that this effect was caused by different burial depth of these deposits.

Paleotemperature

Shackleton and Kennet (1975), Friedman and O'Neil (1977) and Anderson and Arthur (1983) proposed different formulae for calculation of ambient water temperature. However, in this study the Anderson and Arthur (1983) equation was used for calculation of paleotemperature as follows:

$$T = 16.0 - 4.14\,(\delta_c - \delta_w) + 0.13\,(\delta_c - \delta_w)^2$$

Where T is temperature, δ_c is the oxygen isotope ratio for calcite relative to PDB and δ_w is the oxygen isotope ratio for water relative to SMOW.

By using +1.50 per mil for $\delta^{18}O$ for the least altered calcite (lime mud) in all studied samples and -1.2 per mil for the oxygen isotope value for the Upper Jurassic waters (Marshall and Ashton 1980; Price and Sellwood 1994), we calculated 28° C for the ambient water temperature during deposition of the Upper Jurassic limestone of Mozduran Formation in the study area. It showed that the study area during the Late Jurassic time was probably located in a tropical region. This interpretation can be supported by present of ooid, pelloid, coral fragments, evaporite, red and green algae and is similar to observations made by Adabi and Rao (1991).

Elemental analysis

Results: Elemental analysis (Ca, Mg, Fe, Mn, Sr and Na) of the Mozduran Formation limestones are shown in Table 3. These data show that insoluble residue in samples is less than 10% and Ca wt% in calcitic grains ranges from 30 to 40. Mg wt% is also between 0.2 to 1.5 and shows low Mg calcite mineralogy. Sr values in ooids, lime mud, cement and brachiopods range from 110 to 280, 130 to 430, 220 to 410 and 140 to 480 ppm, respectively. Mn in ooids ranges from 360 to 850 ppm, in lime mud from 530 to 2170 ppm, in cement from 150 to 8700 and in brachiopods from 350 to 910 ppm. Fe and Na values are greater than Mn and Sr concentrations. Fe values in ooids, lime mud, cement and brachiopods range from 4360 to 12880, 950 to 7940, 4890 to 11090 and 3090 to 10360 ppm, respectively. Na in ooids varies from 8180 to 18790, in lime mud from 2600 to 6260, in cement from 2770 to 17140 and in brachiopods from 4290 to 31130 ppm.

Average values of trace elements in the studied limestones, without consideration of grain types, are 7946 ppm for Na, 339 ppm for Sr, 6606 ppm for Fe and 1131 ppm for Mn.

Table 3

Discussion: Cross plots of trace elements (Fe, Mn, Na and Sr) versus carbon and oxygen isotopes are shown in figure 8 (A to H). Strontium concentration is much less than recent carbonate values (Milliman 1974). It can be related to meteoric diagenetic effects as well as original mineralogy (low Mg calcite) of carbonates. Original mineralogy can be interpreted from preservation of internal fabric of ooids in the studied samples. Worldwide sea level change of Vail et al. (1991) also correlated to this change of Sr values in this deposit. Na values are close to values in recent carbonates (Milliman 1974). Sr and Na concentration in diagenetic calcites can be controlled by the partition coefficient (less than 1) and low concentration in meteoric waters.

Mn and Fe cross plot (Fig. 8) showed a positive correlation that revealed meteoric diagenetic conditions (Winefield et al. 1994). Increasing concentration of these two elements can be related to the effect of freshwater with higher Mn and Fe values as well as their Partition Coefficient (approximately 15) (e.g. Pingitor et al. 1988, Brand and Veizer 1980). Redox potential also controlled Fe and Mn values in the study area. If the amount of Mn and the Mn/Fe ratio are enough (see Frank et al. 1982) in anoxic condition, then this can lead to luminescence in calcite cements and veins. Amini and Rao (1998) believe siliciclastic influx can increase the Mn and Fe values in shallow marine carbonate environments. In the study samples these are dull and bright

zones under CL, indicating fluctuation of Mn and Fe elements. This could have been caused by the flow of fluids with different compositions and different redox conditions during the cement precipitation.

Fig. 8

Paragenetic sequence

The sequence of diagenetic events in a carbonate system depends on factors such as the sediment itself, grain size and texture, mineralogy, nature of pore-fluid and climate (Tucker and Wright 1990; Tucker 1993; Flugel 2004). Based on petrographic characteristics and geochemical results, diagenetic processes have operated in three different environments (Figs.9 and 10). Early diagenetic stage processes operated in marine and meteoric phreatic environments. Marine diagenetic environments are recognized by first generation nonferroan isopachous cements, micritization and physical compaction. In meteoric phreatic environments, aragonite particles are dissolved and interparticle porosity is generated. In addition, neomorphism and formation of non-ferron, anhedral to subhedral, medium-size dolomite have taken place. Burial diagenetic stage processes affected the Mozduran Formation in deeper and higher temperature area relative to the marine diagenetic stage. At this burial stage, diagenetic processes included cementation (blocky, granular, drusy, poikilotopic), increasing Fe and Mn contents in cements during reducing conditions, physical and chemical compaction (stylolites, increasing grain contacts), dissolution, fracturing and replacement of subhedral to euhedral dolomites. Dolomitization is an important process in this stage, which affected grainstones, void space and veins. Based on the absence of baroque dolomites and sulfide mineralization, burial depth may have not been very much (e.g. Budd 1997; Warren 2006). Relatively coarse and euhedral dolomite crystals in sandstones may have been formed at this stage.

Mechanical and chemical compaction as well as cementation is the dominant porosity modifying agents. Sediment texture and the relative compactability of grains such as pelloid and algal debris may affect the early mechanical compaction history of carbonate sediments of Mozduran Formation. Early cementation and pervasive dolomitization tend to retard the onset and efficiency of chemical compaction. Marine and meteoric processes mostly occur in early stages and shallow burial but physical and especially chemical compaction, fracturing, blocky cementation occur in late stages and deeper part of burial (e.g. Benoit et al 2007). Dolomitization and neomorphism occur in different depth of burial.

Late diagenetic processes affected these sediments after uplifting and formation of fractures by the late Alpain orogenies when the basin was folded and faulted in Miocene time. Some fractures have been filled with sparry calcite. Dissolution and fracturing are the most important processes that helped to create secondary porosity in this interval. Dissolution took place when these rocks were flushed by low-ph meteoric waters, while fracturing is occurred during the late burial diagenetic environment as well as uplifting.

Based on geochemical studies, cements precipitated during the late diagenesis have high amounts of Fe and Mn and less Sr and Na. Stable isotopes also change in different types of cement that are due to different stages of diagenesis. For example, the value of $\delta^{18}O$ decreases from early-to-late diagenetic cements as depth of burial increases. Measured temperature from the lightest oxygen isotope value is about 50° C and based on Kopet-Dagh Basin burial history (Moussavi-Harami and Brenner, 1992), this temperature can be correlated with burial depth about 1300m for Mozduran Formation during Late Jurassic to Early Cretaceous time. Maximum burial depth of Mozduran Formation is calculated about 4000m (Moussavi-Harami and Brenner, 1992). In summary, the study area deposits show different stages of diagenesis in marine, meteoric and burial environments. Most of these processes occurred in burial and meteoric environments.

Fig. 9

Fig. 10

Conclusions

The Mozduran Formation in the Kopet-Dagh basin is mainly composed of carbonate and gradually changes to siliciclastic facies in the easternmost parts of the basin. These sediments were deposited in shallow marine and shoreline environments. Various diagenetic processes affected carbonate and siliciclastic sediments of the Mozduran Formation. These processes include cementation, micritization, dissolution, silicification, neomorphism, compaction (physical and chemical), dolomitization, hematitization and fracturing. These processes occurred in marine, meteoric and burial environments. Temperature of the ambient water during deposition of the Upper Jurassic in the study area was about 28°C, therefore these sediments were probably deposited under tropical climatic conditions that supported by present of chlorozoan assemblages. Maximum

temperature estimated is about 50° C that can be correlated with burial depth about 1300m for Mozduran Formation. Dissolution and fracturing are the important diagenetic processes to create secondary porosity in this interval. We hope, these data can be used in evaluation of reservoir characterization in other parts of this basin as well as similar basins in other parts of the world.

References

ADABI, M.H. and RAO, C.P., 1991, Petrographic and geochemical evidence for original aragonite mineralogy of Upper Jurassic carbonate (Mozduran Formation), Sarakhs Area, Iran: *Sedimentary Geology*, v. 72, p. 253-267.

ADABI, M.H., MOUSSAVI-HARAMI, R., MAHBOUBI A., and SHEMIRANI, A., 2006, Petrography, elemental and isotope variation of rudist biostrome of Maastrichtian platform in east Kopet-Dagh basin, NE Iran: *Journal of Geological Society of Iran*, v. 1, p. 1-10.

ADACHI, N., EZAKI, Y., and LIU, J., 2004, The origins of peloids immediately after the end-Permian extinction, Guizhou Province, South China: *Sedimentary Geology*: v. 164, p. 161-178.

ADAMS, A.E., and MACKENZIE, W.S., 1998, A color atlas of carbonate sediments and rocks under the microscope: *Manson Publishing, London,* 180p.

AESHAR-HARB, A., 1979, The stratigraphy, tectonics and petroleum geology of the Kopet-Dagh Region, Northern Iran: PhD thesis, Imperial College of Sciences, University of London, United Kingdom, 316p.

AESHAR-HARB, A., 1994, Geology of the Kopet-Dagh: Tehran, *Geological Survey of Iran*, 265p.

AHMAD, A.H.M. and BHAT, G.M., 2006, Petrofacies, provenance and diagenesis of the Dhosa Sandstone Member (Chari Formation) at Ler, Khachchh sub-basin, western India. *Asian Journal of Earth Science*, XX, p. 1-16.

ALAVI, M., VAZIRI., H., SEYED-EMAMI, K., and LASEMI, Y., 1997, The Triassic and associated rocks of the Aghdarband areas in central and northeastern Iran as remnant of the southern Turanian active continental margin: *Geological Society of America Bulletin*, v. 109, p. 1563-1575.

ALSHARHAN, A.S. and KENDALL, C.G.S.T.C., 2003, Holocene coastal carbonates and evaporites of the southern Arabian Gulf and their ancient analogues: *Earth Science Review*, v. 61, p. 191-243.

AMINI, Z. and RAO, C.P., 1998, Depth and latitudinal characteristic of sedimentological and geochemical variables in temperate shelf carbonates, eastern Tasmania, Australia: *Carbonates and Evaporites*, v. 13, p. 142-156.

ANDERSON, T.F. and ARTHUR, M.A., 1983, Stable isotopes of oxygen and carbon and their application to sedimentologic and paleoenvironmental problems, In: Arthur MA, Anderson TF, Kaplan IR, Veizer J, Land L (eds.) Stable Isotopes in Sedimentary Geology: *SEPM Short Course Notes 10*, Section, 1.1, p. 1-151.

BATHURST, R.G.C., 1975, Carbonate sediments and their diagenesis: Second Edition, *Developments in Sedimentology 12, Elsevier Amsterdam*, 658p.

BENOIT, V., LAURENT, E., PASCAL, H., and Jean-paul, L., 2007, Geodynamic control on carbonate digenesis: Petrographic and isotope investigation of the Upper Jurassic formations of the Paris Basin (France): *Sedimentary Geology*, v. 197, p. 267-289.

BERBERIAN, M. and KING, G.C.P., 1981, Toward paleogeographic and tectonic evolution of Iran: *Canadian Journal of Earth Sciences*, v. 18, p. 210-265.

BRAND, U. and VEIZER, J., 1980, Chemical diagenesis of the multi component carbonate system-1: trace elements: *Journal of Sedimentary Petrology*, v. 50, p. 1219-1236.

BUDD, D.A., 1997, Cenozoic dolomites of Carbonate Island: Their attributes and origin: *Journal of Earth Science Review*, v. 42, p. 1-47.

BURCHETTE, T.P., WRIGHT, V.P., and FAULKNER, T.J., 1990, Oolithic sand body depositional models and geometries, Mississippian of southwest Britain: implication in carbonate ramp settings. Sedimentary Geology 68, 87-115.

CAROLS, L.J., 2002, Diagenetic history of the Upper Jurassic Smackover Formation and its effects on reservoir properties: Vocation Field, Manila Sub-Basin, Eastern Gulf Coastal Plain. Gulf Coast Association of Geological Societies Transactions, v. 52, p. 631-644.

CHOQUETTE, P.W. and JAMES, N.P., 1987, Diagenesis in limestones-3. The deep burial environment: *Geoscience. Canada*, v. 14, p. 3-35.

COFFEY, B.P. and READ, J.F., 2004, Mixed carbonate-siliciclastic sequence stratigraphy of Paleogene transition zone continental shelf, southeastern USA: *Sedimentary Geology*, v. 166, p. 21-57.

Dickson JAD (1966) Carbonate identification and genesis as revealed by staining: *Journal of Sedimentary Petrology:* v. 36, p. 441-505.

EHRENBERG, S.N., PICKARD, N.A.H., SVANA, T.A., and OXTOBY, N.H., 2002, Cement geochemistry of photozoan carbonate strata (Upper Carboniferous-Lower Permian), Finnmark Carbonate Platform, Brents Sea: *Journal of Sedimentary Research*, v. 72, p. 95-115.

FLUGEL, F., 2004, Microfacies of carbonate rocks- analysis, interpretation and application, *Springer- Verlag, Berlin*, 967 p.

FORTUIN, A.R. and KRIJGMAN, W., 2003, The Messinian of the Nijar basin (SE Spain): sedimentation, depositional environments and paleogeographic evolution: *Sedimentary Geology*, v. 160, p. 213-242.

FOUKE, B.W., ZERKLE, A.L., ALVAREZ, W., POPE, K.O., OCAMPOS, A.G., WACHTMAN, R.J., NISHIMURA, J.M.G., CLAEYS, P., and FISCHER, A.G., 2002, Cathodoluminescence petrography and isotope geochemistery of KT impact eject deposited 360 km from the Chicxulub Cracter, at Albion Island, Belize: *Sedimentary Geology*, v. 49, p. 117-138.

FRANK, J.R., CARPENTER, A.B., and OGLESBY, T.W., 1982, Cathodoluminscence and composition of calcite cement in the Taum Sauk Limestone (Upper Cambrian), South Missouri: *Sedimentary Geology*, v. 52, p. 631-638.

FRANK, T.C., LOHMANN, K.C., and MEYERS, W.J., 1995, Chronostratigraphic significance of cathodoluminescence zoning is syntaxial cement: Mississippian Lake Vally Formation, New Mexico: *Sedimentary Geology*, v. 105, p. 29-50.

FRIEDMAN, I. and O'NEIL, J.R., 1977, Compilation of stable isotope fractionation factors of geochemical interest: in Fleischer, M., (Ed), Data of Geochemistry. 6th edition: U.S. *Geological Survey Prof. Paper*, 440-KK, p. 1-12.

HOLZ, M., 2003, Sequence stratigraphy of lagoonal estuarine system-an example from the Lower Permian Rio Benito Formation, Parana basin, Brazil: *Sedimentary Geology*, v. 102, p. 305-331.

HUDSON, J.D., 1977, Stable isotopes and limestone lithification: *Journal of Geological Society of London*, v. 133, p. 637-660.

JAMES, N.P. and CHOQUETTE, P.W., 1983, Diagenesis,6, Limestones-the sea floor diagenetic environment: *Geoscience Canada*, v. 10, p.162-179.

KIM, Y. and LEE, Y.I., 2004, Diagenesis of shallow marine sandstones, the Lower Ordovician Dongjeom Formation, Korea: response to relative sea-level changes: *Journal of Asian Earth Sciences*, v. 23, p. 235-245.

KYSER, T.K., JAMES, N.P., and BONE, I., 2002, Shallow burial dolomitization of Cenozoic cool water limestone, southern Australia. Geochemistry and origin: *Journal of Sedimentary Research*, v. 72, p. 146-157.

LOHMANN, K.C., 1988, Geochemical patterns of meteoric diagenetic systems and their application to studies of paleokarst: In James NP, Chaquette PW (eds.), Paleokarst: New York, *Springer-Verlag, New-York*, p. 58-80

MACAULAY, G.I., BECKETT, D.B., BRAITHWAITE, K., BLIEFNICK, D., and PHIPS, B.M., 2001, Constrains on diagenesis and reservoir quality in the fractured Hasdrabal Field, Offshore Tunisia: *Journal of Petroleum Geology*, v. 24, p. 55-78.

MACHENT, P.G., TAYLOR, K.G., MACQUAKER, J.H., and MARSHALL, J.D. 2007, Pattern of early post–depositional and burial cementation in distal shallow marine sandstones: Upper Cretaceous Keniworth Member, Book Cliffs, Utah, USA: *Sedimentary Geology*, v. 198, p. 125-145.

MAHBOUBI, A,, MOUSSAVI-HARAMI, R., YAHYA-SHAYBANI, V., NAJAFI, M., and GONZALEZ, L., 2004, Petrographic and geochemical evidence for paragenetic sequence interpretation of the Lower Cretaceous limestones in the eastern Binalood Mountain Range, NE Iran*: Iranian International Journal of Science*, v. 5(2), p. 181-201.

MAHBOUBI, A., MOUSSAVI-HARAMI, R., AGHAEI, A., ALETAHA, H., 2006, Sequence Stratigraphy and Palaeogeography of the Upper Jurassic reservoir equivalent along the outcrop belt in the Agh-Darband area, northeastern Iran: The 6th International Conference on the Geology of the Middle East, 20-23 March 2006, Al-Ain, UAE, p. 104

MARSHALL, J.D. and ASHTON, M., 1980, Isotopic and trace element evidence for submarine lithification of hardground in Jurassic of England. *Sedimentology*, v. 27, p. 271-289.

MARTIN-CHIVELET, J., RAMIREZ DEL POZO, J., TRONCHETTI, G., BABINOT, J.F., 1995, Palaeoevironmet and evolution of the upper Maastrichtian platform in the Betic continental margin, SE Spain: *Palaeogeography, Palaeoclimatology, Palaeoecology*, v.119, p. 169-186.

MARSHALL, D.J., 1988, Cathodoluminescence of Geological Materials. Unwin Hyman, Boston, 146p.

MEYERS, W.J., 1989, Trace element and isotope geochemistry of zoned calcite cements, Lake Valley Formation (Mississippian,New Mexico). Insights from Water-rock interaction modeling*: Sedimentary Geology*, v. 65, p. 355-370.

MIALL, A.D., 1997, The geology of stratigraphic sequences: *Speringer-verlag, Berlin*, 433p.

MILLIMAN, J.D., 1974, Marine carbonates: *Springer-Verlag, New York*, 375p.

MORSE, J.W. and MACKENZIE, F.T., 1990, Geochemistry of sedimentary carbonates: *Elsevier, New York*, 707p.

MILLIMAN, J.D. and MULLER, J., 1977, Characteristics and genesis of shallow-water and deep-sea limestone: Anderson, NR, Malahoff A (eds) the fate of fossil fuel CO_2 in the oceans, New York, Plenum Press, p. 655-672.

MOUSSAVI-HARAMI, R., 1989, Depositional history of Upper Jurassic (Oxfordian-Kimmeridgian) carbonates and evaporites in northeastern Iran (abs.), Proceeding of the 28th International Geological Congress, Washington DC, 2, 471p.

MOUSSAVI-HARAMI, R. and BRENNER, R.L., 1992, Geohistory analysis and petroleum reservoir characteristics of Lower Cretaceous (Neocomian) sandstone, eastern portion of Kopet-Dagh basin, northeast Iran: *American Association of Petroleum Geologist Bulletin,* v. 76, p. 1200-1208.

NELSON, C.S. and SMITH, A.M., 1996, Stable oxygen and carbon isotopes composition fields for skeletal and diagenetic components in New Zealand Cenozoic non-tropical carbonate sediments and limestones: A synthesis and review. New Zealand, *Journal of Geology and Geophysics*, v.39, p.93-107.

PINGITORE, N.E., EASTMAN, M.P., SANDIDGE, M., ODEN, K., FREIHA, B., 1988, The coprecipitation of manganese (II) with calcite, and experimental study: *Marine Chemistry,* v. 25, p. 107-120.

PRICE, G.D. and SELLWOOD, B.W., 1994, Palaeotemprature indicated by Upper Jurassic (Kimmeridgian-Tithonian) fossils from Mallorca determined by oxygen isotope composition: *Palaeogeography, Palaeoclimatolology, Palaeoecolology,* v. 110, p. 1-10.

RAHIMPOUR-BONAB, H., BONE, Y., and MOUSSAVI-HARAMI, R., 1997, Stable isotopes aspects of modern molluska, brachiopods and marine cements from cool-water carbonate, Lacepede Shelf, South Australia: *Geochimica et Cosmochimica Acta,* v. 61, p. 207-218.

RUTTNER, A.W., 1993, Southern borderland of Triassic Laurasia in northeast Iran: *Geology Rund,* v. 82, p. 110-120.

SANDERS, D. and HOFLING, R., 2000, Carbonate deposition in mixed siliciclastic-carbonate environments on top of an orogenic wedge (Late Cretaceous, Northern Calcareous Alps, Austria): *Sedimentary Geology,* v.137, p. 127-146.

SCHNEIDER, A.J., WALL, H.D., and BECHSTADT, T., 2004, Magnetic susceptibility variation in carbonates of the La Vid Group (Cantabrian Zone, NW-Spain) related to burial diagenesis: *Sedimentary Geology,* v. 166, p. 73-88.

SHAKLETON, N.J. and KENNETT, J.P., 1975, Palaeotemprature history of the Cenozoic and the initiation of Antartic glaciation: oxygen and carbon isotope analysis in DSDP Sites 277-279 and 281. Initiate report DSDP XX1X, p. 743-755.

SIBLEY, D.F. and GREEG, J.M., 1987, Classification of dolomite rock textures: *Journal of Sedimentary Petrology,* v. 57, p. 967-975.

TAMURA, T. and MASUDA, F., 2003, Shallow-marine fan delta slope deposits with large-scale cross-stratification: the Plio-Pleistocene Zaimokuzawa Formation in the Ishikari Hills, northern Japan: *Sedimentary Geology*, v. 158, p.195-207.

TUCKER, M.E., 1988, Techniques in Sedimentology, Blackwells, Oxford, 394p.

TUCKER, M.E. and WRIGHT, V,P., 1990, Carbonate Sedimentology. Black-Well, Oxford, 482p.

TUCKER, M.E., 1993, Carbonate diagenesis and sequence stratigraphy, in: Wright VP (Ed.) Sedimentary Review, Black Wells, Oxford, p. 208-226.

VAIL, P.R., AUDEMART, F., BOWMAN, S,A., EINSER, P.N., and PEREZ CRUZ, G., 1991, The stratigraphic significances of tectonics, eustasy and sedimentology an overview. In: Einsle G, Ricken W, Seilacher A (Eds.), Cycles and Events in Stratigraphy: Springer-Verlag, Berlin, p. 617-659.

VINCENT, B., EMMANUEL, L., HOUEL, P., LOREAU, J., 2007, Geodynamic control on carbonate diagenesis: Petrographic and isotopic investigation of the Upper Jurassic Formations of the Paris Basin (France): *Sedimentary Geology*, v. 197, p. 267-289.

WARREN, J., 2006, Evaporites, Sediments, Resource and Hydrocarbons, Springer-Verlag, 1035p.

WEIBLE, R., FRIIS, H., 2004, Opaque minerals as keys for distinguishing oxidizing and reducing diagenetic conditions in the lower Triassic Bunter Sandstone, North German Basin: *Sedimentary Geology*, p.1-21.

WINEFIELD, P.R., NELSON, C.S., and HODDER, A.P.W., 1996, Discriminating temperate carbonates and their diagenetic environments using bulk elemental geochemistry: a reconnaissance study based on New Zealand Cenozoic limestones: *Carbonates and Evaporites*, v. 11, p. 19-31

YECHIELI, Y. and WOOD, W.W., 2003, Hydrogeologic processes in saline systems: playas, sabkhas, and saline lakes: *Earth Science Review*, v. 58, p. 343.365.

Figure captions

Figure 1: Location map of the study area. Letters show the location of measured stratigraphic sections. North Shurab (A), Kal-e-Shahmohammad 2 (B), Shurab (C), Kal-e-ShahMohammad 1 (D), Kol-e-Malekabad (E), Kal-e-Karab (F), Derazab (G), Karizak (H).

Figure 2: Microfacies correlation of study area. The above box shows locality of measured stratigraphic sections at Mozduran Formation outcrops.

Figure 3: Conceptual depositional model of Upper Jurassic Mozduran Formation showing spatial relationship of facies associations A- G (After Mahboubi et al., 2006) .

Figure 4: Photomicrographs show the effect of diagenetic processes in the studied samples. (A) micritization that affected echinoderm fragment margin. (B) Ispachous (a) and granular calcite cements (b) in grainstone. Fracture filling in carbonate grains with sparry calcite cement. (C) Coarse crystalline blocky calcite. (D) Poikilotopic cement in ooid grainstone. (E) Syntaxial cement around echinoderm fragments. (F) stylolite in grainstone. (G) Compaction that resulted from overburden pressure**.**

Figure 5: Photomicrographs of diagenetic processes: (A) Dissolution in limestones. (B) Aggradational neomorphism in mudstones. (C) Fractures in mudstones have been filled by calcite cement. (D) Overgrowth silica cement around quartz grain. (E) Calcite (a) and dolomite cements (b) in sandstones. (F) Fine crystalline dolomite (D_1 type). (G) Medium crystalline dolomites replacing echinoderm fragments (D_2 type). (H) Pore filling coarse crystalline dolomites (D_3 type).

Figure 6: Photomicrographs showing fracture filling with calcite crystals. (A) Vein filled by coarse crystalline calcite (PPL). (B) The same vein as A under CL. Dull and bright zoning indicates differences in composition of water during precipitation of calcite cement. (C) Pore and fracture filling coarse crystalline dolomites (PPL). Cloudy center and bright margin is very obvious in these dolomites. (D) Dolomite crystals under CL. Different luminescence in dolomites show that they formed in different conditions. For example red luminescence in dolomite crystals shows burial and redox conditions during replacement.

Figure 7: Comparison between $\delta^{18}O$ and $\delta^{13}C$ value of study samples with Recent whole sediment in warm shallow marine water and Recent warm shallow marine water sediments and skeletons. This trend is similar to inverted J- trend of Lohmann (1988). It indicates influence of meteoric diagenesis.

Figure 8: Cross-plots of $\delta^{18}O$ versus Fe, Mn, Na and Sr in carbonate samples of the Mozduran Formation in the study area (A, B, C and D). High value of Fe and low value of $\delta^{18}O$ and Sr indicating influence of meteoric diagenesis. Cross-plots of $\delta^{13}C$ versus Fe, Mn, Na and Sr in carbonate samples of the study area (E, F, G and H). High value of Fe and low value of $\delta^{13}C$ and Sr indicating influence of meteoric diagenesis. High values of Na indicating high salinity and evaporation during the formation of carbonates.

Figure 9: Paragenetic sequence of the Mozduran Formation limestones in the study area.

Figure 10: Paragenetic sequence of the Mozduran Formation siliciclastics in the study area.

Tables

Table1. Summary of lithofacies types Mozduran Formation in the study area

Table2. Results of carbon and oxygen stable isotopes analysis for the Mozduran Formation limestones.

Table3. Results of elemental analysis for limestone samples.

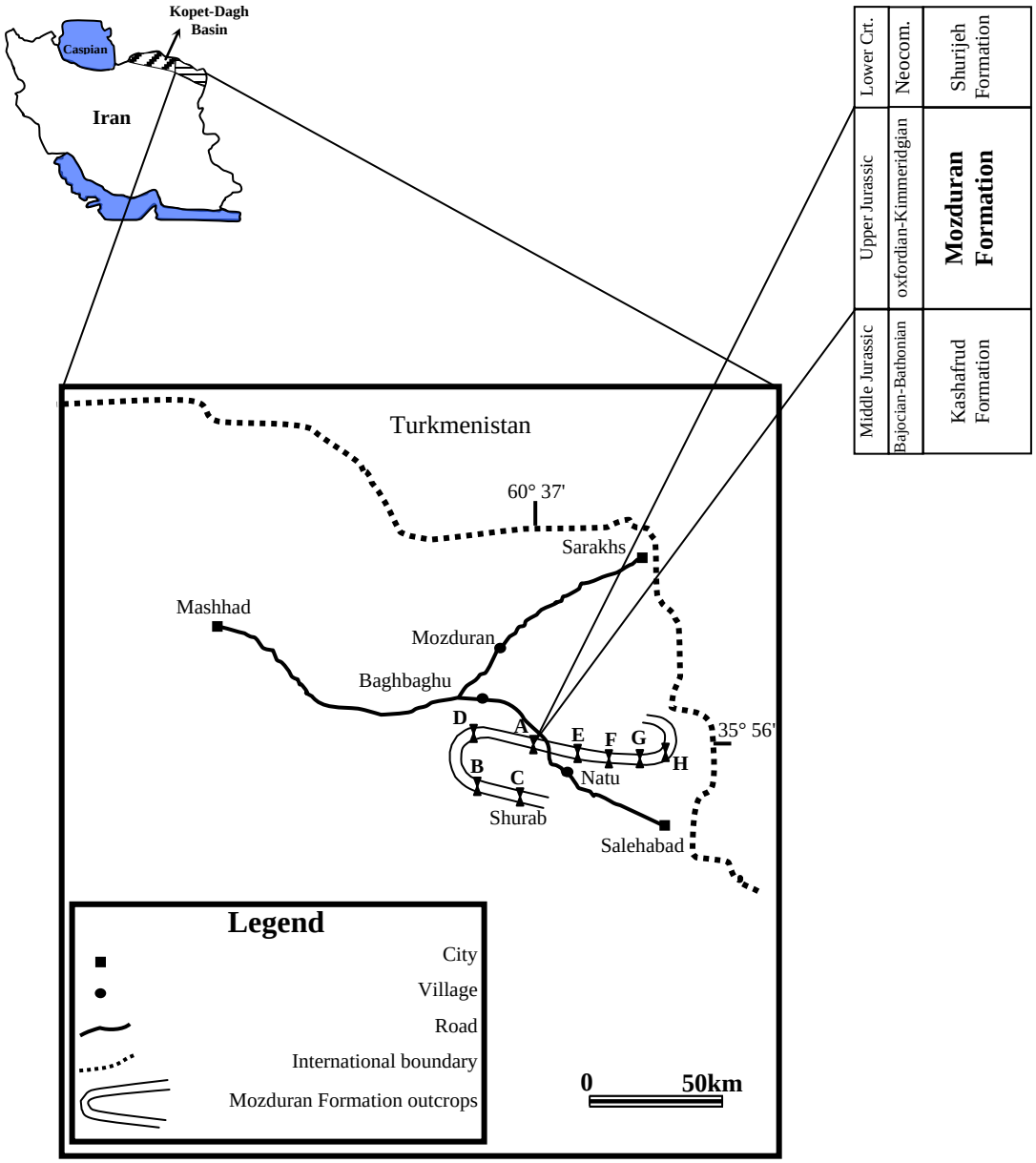
Kopet-Dagh Basin
Caspian
Iran
Turkmenistan
60° 37'
35° 56'
Sarakhs
Mashhad
Mozduran
Baghbaghu
Natu
Shurab
Salehabad
A
B
C
D
E
F
G
H
Legend
City
Village
Road
International boundary
Mozduran Formation outcrops
0
50km
Lower Crt.
Neocom.
Shurijeh Formation
Upper Jurassic
oxfordian-Kimmeridgian
Mozduran Formation
Middle Jurassic
Bajocian-Bathonian
Kashafrud Formation

Fig. 1

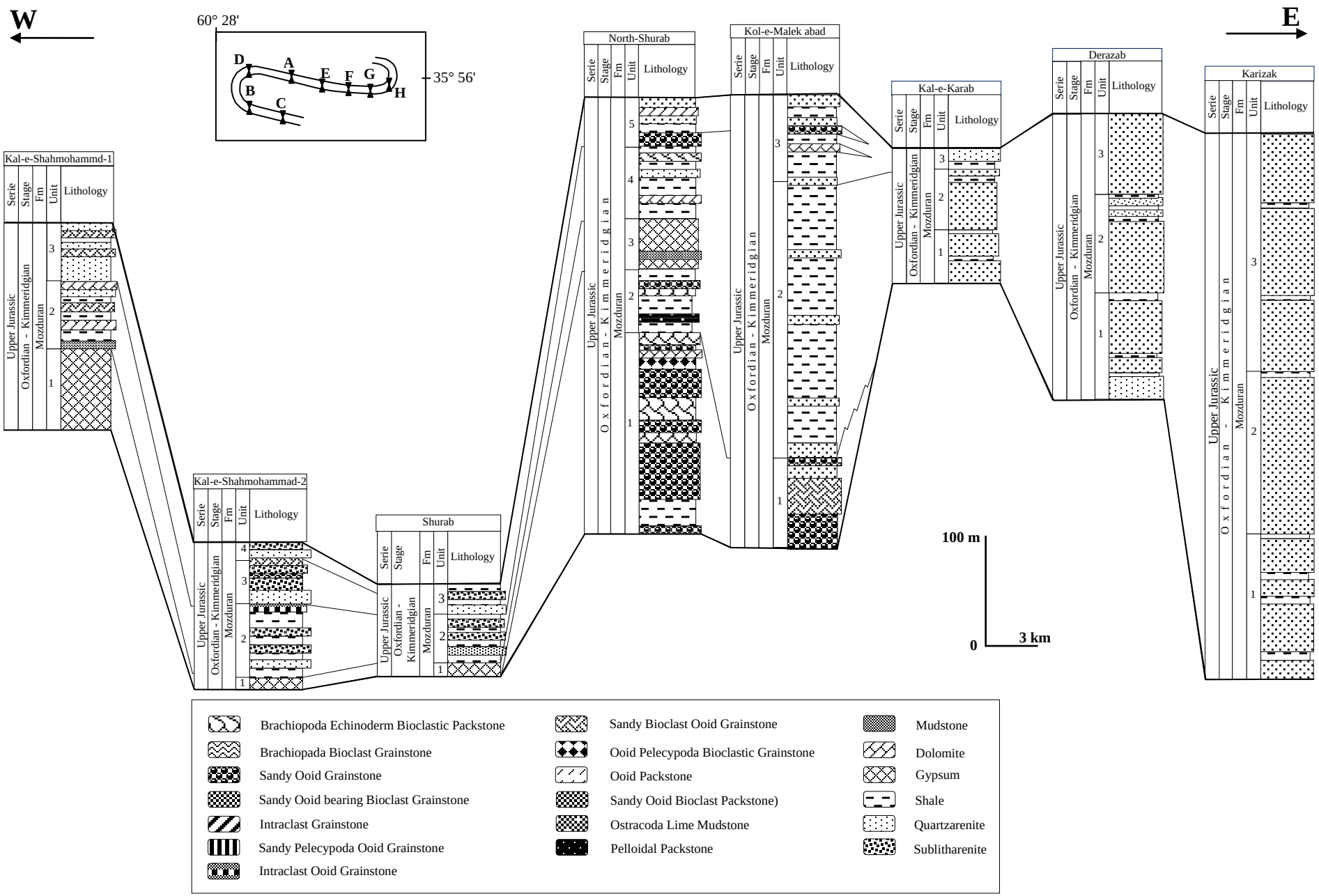
W
E
60° 28'
35° 56'
D
A
E
F
G
H
B
C
Kal-e-Shahmohammd-1
Kal-e-Shahmohammad-2
Shurab
North-Shurab
Kol-e-Malek abad
Kal-e-Karab
Derazab
Karizak
Serie
Stage
Fm
Unit
Lithology
Upper Jurassic
Oxfordian - Kimmeridgian
Mozduran
100 m
0
3 km
Brachiopoda Echinoderm Bioclastic Packstone
Brachiopada Bioclast Grainstone
Sandy Ooid Grainstone
Sandy Ooid bearing Bioclast Grainstone
Intraclast Grainstone
Sandy Pelecypoda Ooid Grainstone
Intraclast Ooid Grainstone
Sandy Bioclast Ooid Grainstone
Ooid Pelecypoda Bioclastic Grainstone
Ooid Packstone
Sandy Ooid Bioclast Packstone)
Ostracoda Lime Mudstone
Pelloidal Packstone
Mudstone
Dolomite
Gypsum
Shale
Quartzarenite
Sublitharenite

Fig. 2

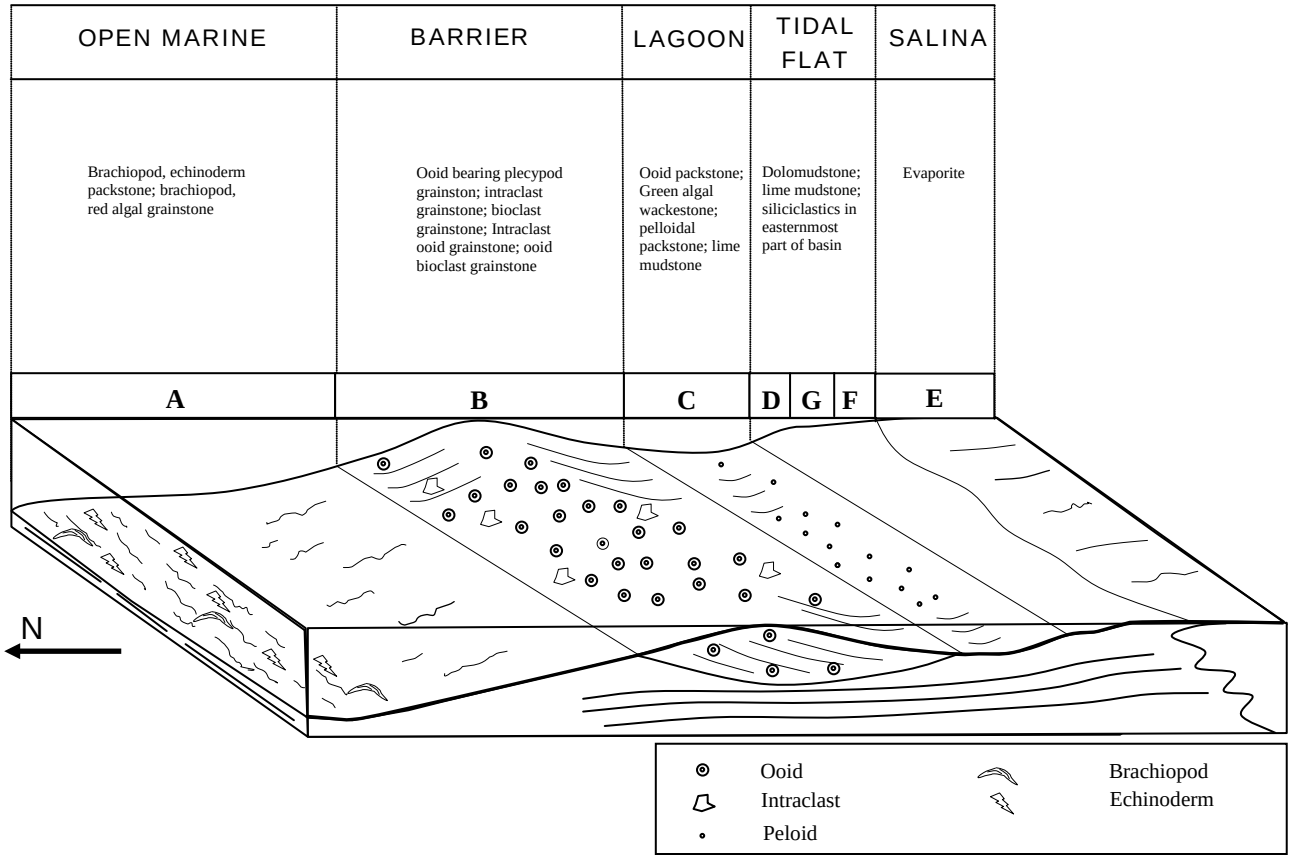
OPEN MARINE
BARRIER
LAGOON
TIDAL FLAT
SALINA
Brachiopod, echinoderm packstone; brachiopod, red algal grainstone
Ooid bearing plecypod grainston; intraclast grainstone; bioclast grainstone; Intraclast ooid grainstone; ooid bioclast grainstone
Ooid packstone; Green algal wackestone; pelloidal packstone; lime mudstone
Dolomudstone; lime mudstone; siliciclastics in easternmost part of basin
Evaporite
A
B
C
D
G
F
E
N
Ooid
Intraclast
Peloid
Brachiopod
Echinoderm

Fig. 3

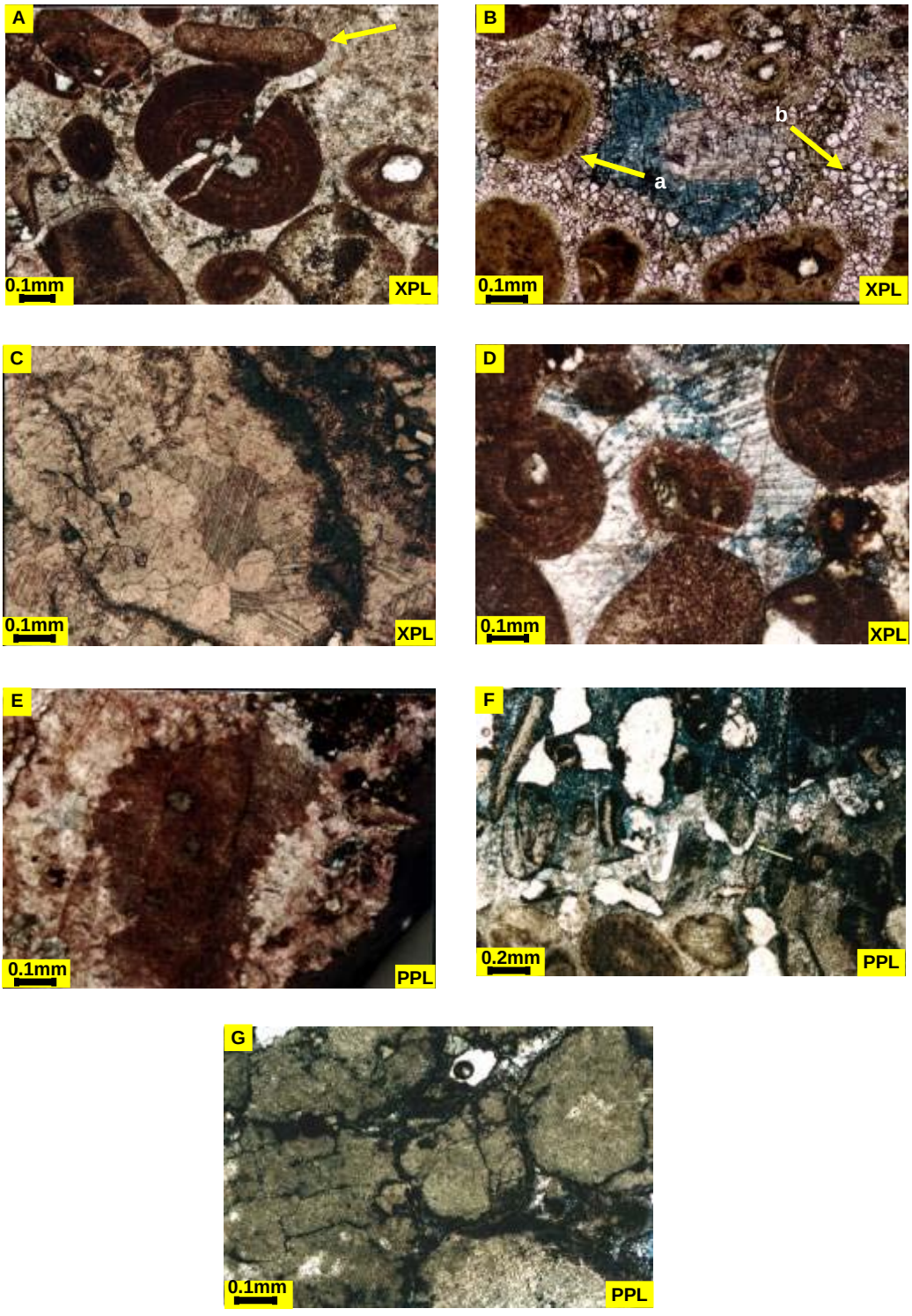
A
0.1mm
XPL
B
b
a
0.1mm
XPL
C
0.1mm
XPL
D
0.1mm
XPL
E
0.1mm
PPL
F
0.2mm
PPL
G
0.1mm
PPL

Fig. 4

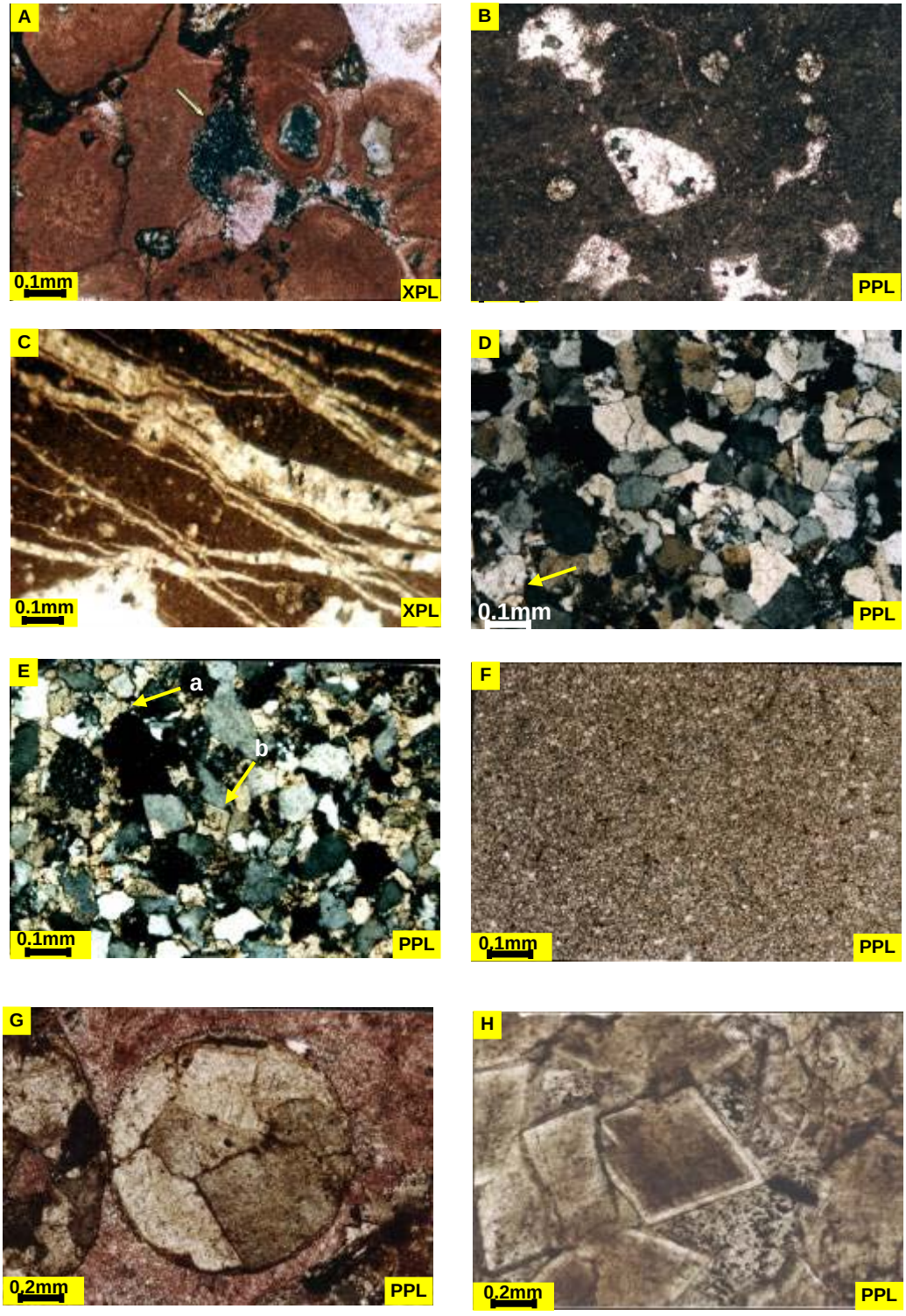
A
0.1mm
XPL
B
PPL
C
0.1mm
XPL
D
0.1mm
PPL
E
a
b
0.1mm
PPL
F
0.1mm
PPL
G
0.2mm
PPL
H
0.2mm
PPL

Fig. 5

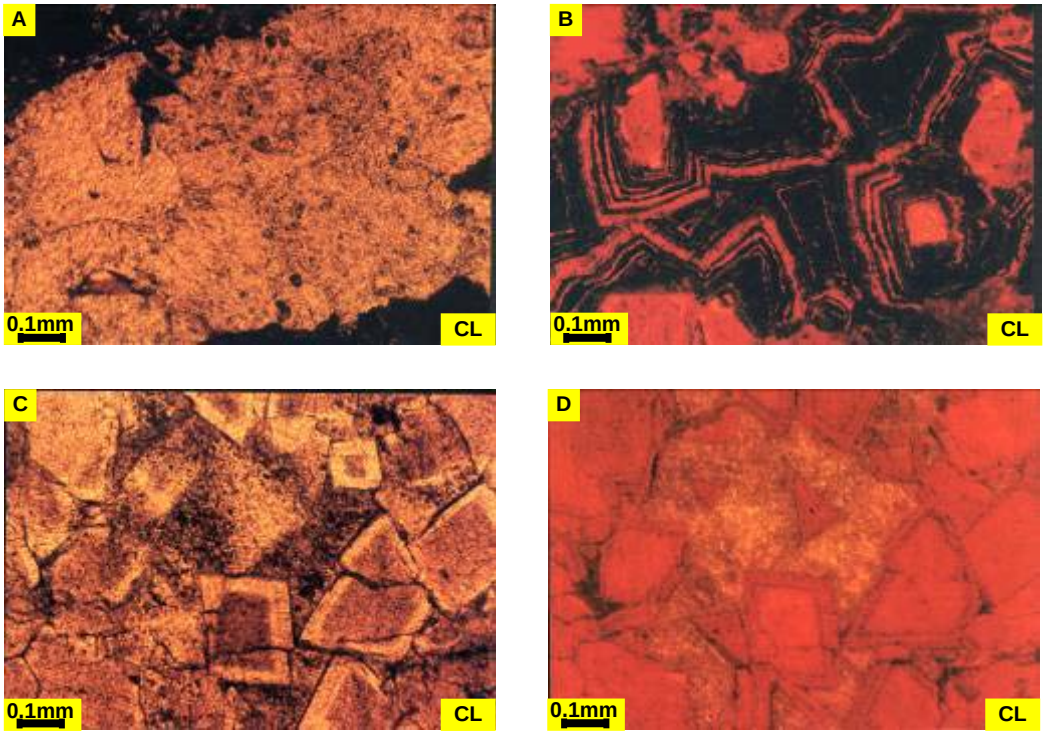

Fig. 6

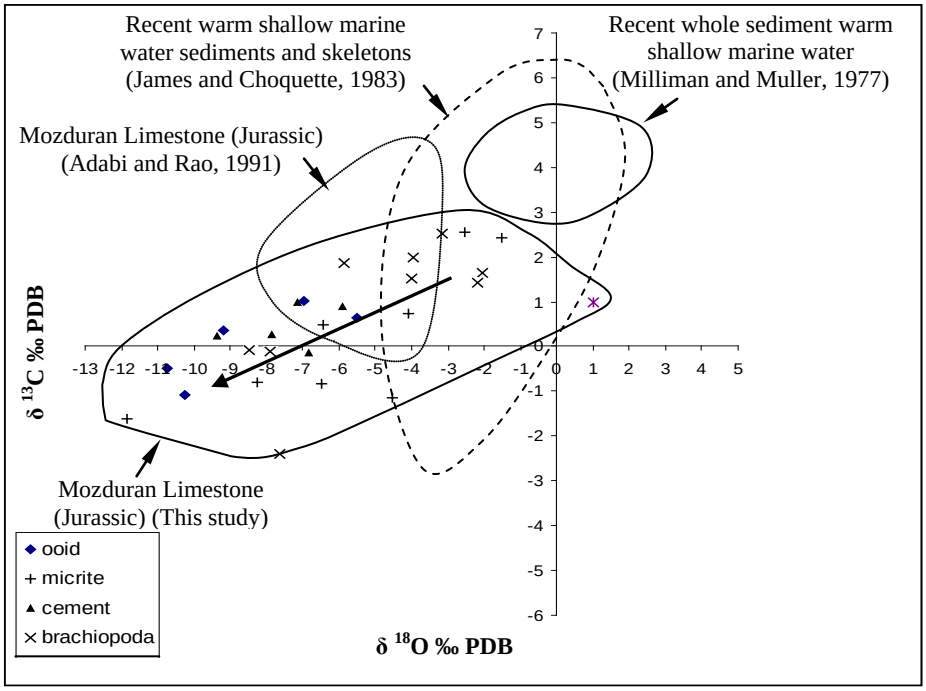
Recent warm shallow marine water sediments and skeletons (James and Choquette, 1983)
Recent whole sediment warm shallow marine water (Milliman and Muller, 1977)
Mozduran Limestone (Jurassic) (Adabi and Rao, 1991)
Mozduran Limestone (Jurassic) (This study)
ooid
micrite
cement
brachiopoda
δ 13C ‰ PDB
δ 18O ‰ PDB

Fig. 7

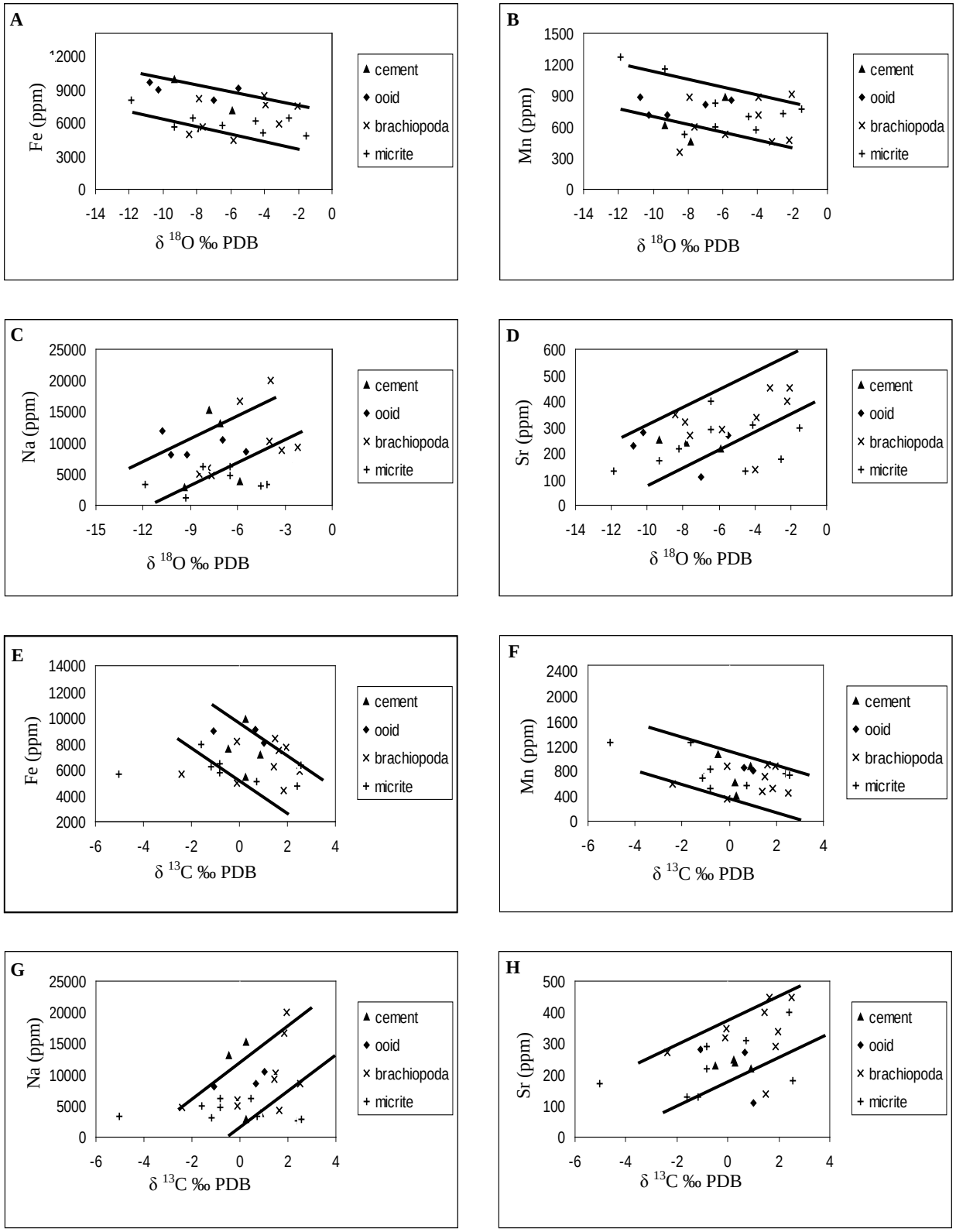
A
Fe (ppm)
12000
9000
6000
3000
0
-14 -12 -10 -8 -6 -4 -2 0
δ 18O ‰ PDB
cement
ooid
brachiopoda
micrite
B
Mn (ppm)
1500
1200
900
600
300
0
-14 -12 -10 -8 -6 -4 -2 0
δ 18O ‰ PDB
cement
ooid
brachiopoda
micrite
C
Na (ppm)
25000
20000
15000
10000
5000
0
-15 -12 -9 -6 -3 0
δ 18O ‰ PDB
cement
ooid
brachiopoda
micrite
D
Sr (ppm)
600
500
400
300
200
100
0
-14 -12 -10 -8 -6 -4 -2 0
δ 18O ‰ PDB
cement
ooid
brachiopoda
micrite
E
Fe (ppm)
14000
12000
10000
8000
6000
4000
2000
-6 -4 -2 0 2 4
δ 13C ‰ PDB
cement
ooid
brachiopoda
micrite
F
Mn (ppm)
2400
2000
1600
1200
800
400
0
-6 -4 -2 0 2 4
δ 13C ‰ PDB
cement
ooid
brachiopoda
micrite
G
Na (ppm)
25000
20000
15000
10000
5000
0
-6 -4 -2 0 2 4
δ 13C ‰ PDB
cement
ooid
brachiopoda
micrite
H
Sr (ppm)
500
400
300
200
100
0
-6 -4 -2 0 2 4
δ 13C ‰ PDB
cement
ooid
brachiopoda
micrite

Fig. 8

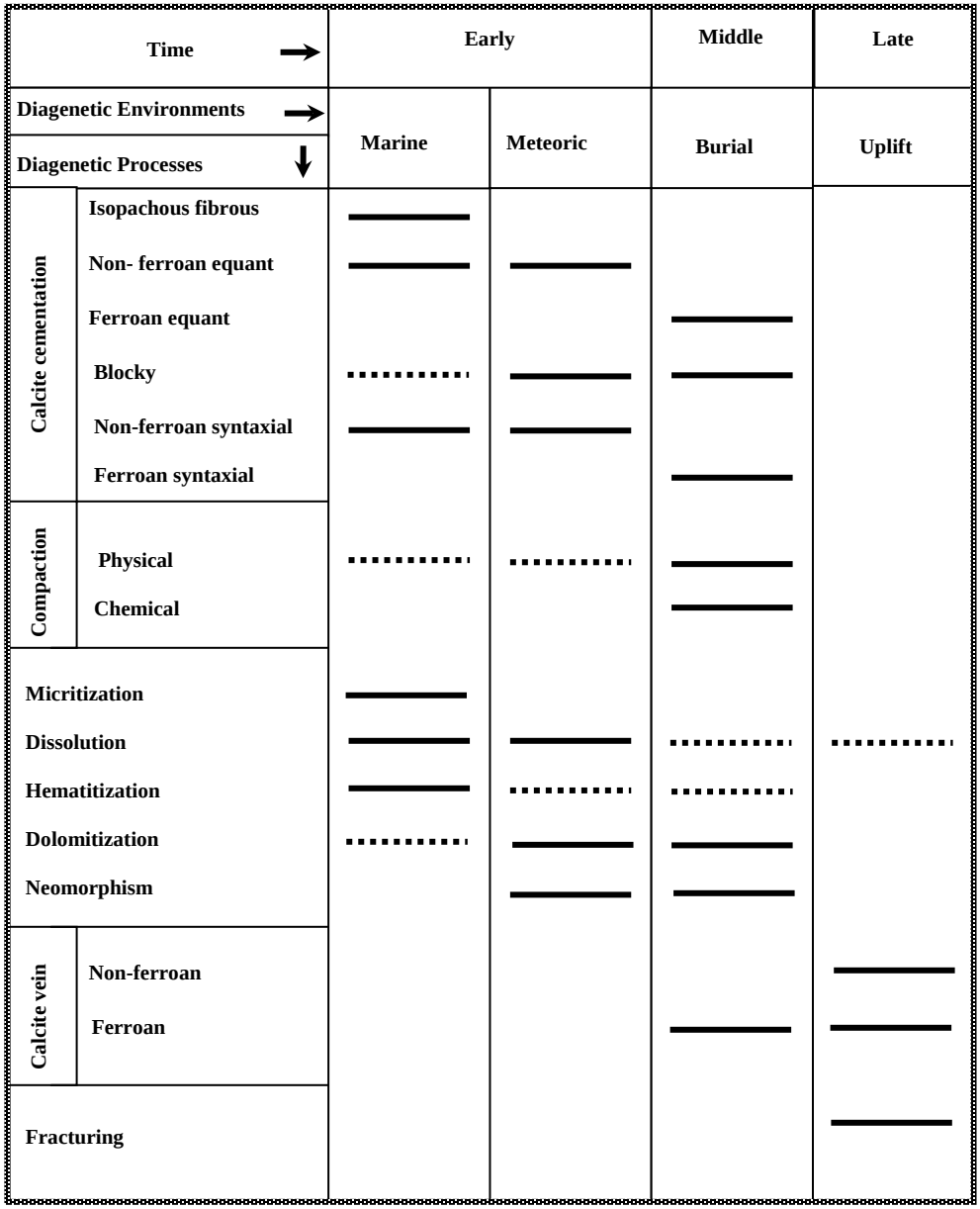
Time
Early
Middle
Late
Diagenetic Environments
Diagenetic Processes
Marine
Meteoric
Burial
Uplift
Calcite cementation
Isopachous fibrous
Non- ferroan equant
Ferroan equant
Blocky
Non-ferroan syntaxial
Ferroan syntaxial
Compaction
Physical
Chemical
Micritization
Dissolution
Hematitization
Dolomitization
Neomorphism
Calcite vein
Non-ferroan
Ferroan
Fracturing

Fig. 9

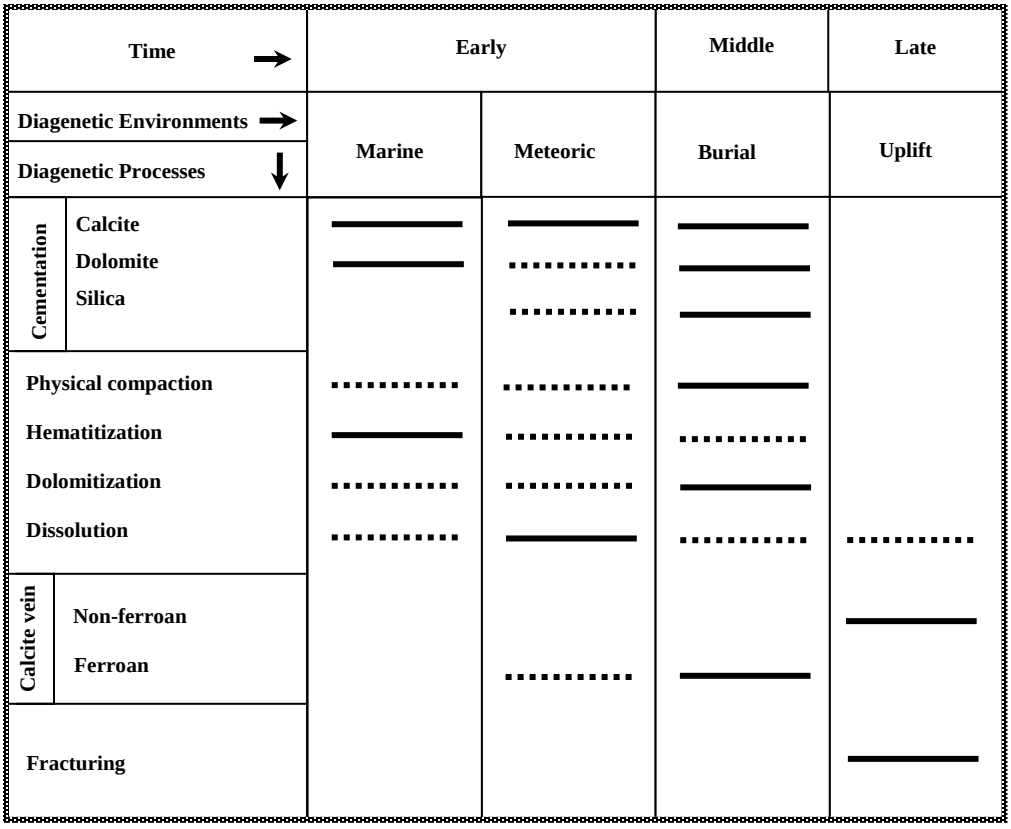
Time
Early
Middle
Late
Diagenetic Environments
Diagenetic Processes
Marine
Meteoric
Burial
Uplift
Cementation
Calcite
Dolomite
Silica
Physical compaction
Hematitization
Dolomitization
Dissolution
Calcite vein
Non-ferroan
Ferroan
Fracturing

Fig. 10

Microfacies types	Microfacies name	Skeletal components	Non skeletal components	Interpretation
A_1	Bioclastic packstone	Brachiopod, Echinoderm, Bivalve, Bryozoan	Intraclast	Open marine
A_2	Bioclastic grainstone	Brachiopod, Bivalves	Ooid, Intraclast	Open marine
B_1	Sandy bioclast grainstone bearing ooid	Brachiopod, Echinoderm, Bivalve, Gastropod, Green algae	Ooid, Intraclast	Barrier
B_2	Sandy bioclast ooid grainstone	Brachiopod, Echinoderm, Bivalve	Ooid, Intraclast	Barrier
B_3	Ooid bioclast grainstone	Bivalve	Ooid, Intraclast	Barrier
B_4	Intraclast grainstone	Echinoderm, Bryozoan	Ooid, Intraclast	Barrier
B_5	Intraclast ooid grainstone	Bivalve, Echinoderm, Gastropod	Ooid, Intraclast	Barrier
B_6	Bioclast ooid grainstone	Bivalve, Echinoderm, Gastropod, Brachiopod, Bryozoan, Green algae	Ooid, Intraclast, Peloid	Barrier
B_7	Sandy ooid grainstone	Bivalve, Gastropod, Brachiopod, Milliolid	Ooid, Intraclast, Peloid	Barrier
C_1	ooid packstone	Bivalve, Gastropod, Milliolid	Ooid, Peloid	Lagoon
C_2	Sandy ooid bioclast packstone	Bivalve, Gastropod, Milliolid	Ooid, Peloid, Intraclast	Lagoon
C_3	Ostracoda mudstone	Ostracoda	Peloid	Lagoon
C_4	Peloidal packstone	-	Peloid	Lagoon
D_1	Mudstone	-	-	Tidal flat
D_2	Dolostone	-	-	Tidal flat
G	Shale	-	-	Tidal En.
F	Sandstone	-	-	Tidal dominated shoreline
E	Gypsum	-	-	Salina

Table 1

Sample No.	δ ^{13}C ‰ PDB	δ ^{18}O ‰ PDB
13(ooid)	0.65	-5.51
49A(ooid)	-1.809	-10.25
65(ooid)	0.36	-9.2
1B-A(ooid)	-0.48	-10.76
20A(ooid)	1.00	-6.98
66(micrite)	0.47	-6.45
97(micrite)	-0.81	-8.24
100(micrite)	2.41	+1.50
105(micrite)	0.72	-4.11
106(micrite)	2.56	-2.52
25B(micrite)	-0.83	-6.46
33B(micrite)	-5.04	-9.32
36B(micrite)	-1.61	-11.86
43B(micrite)	-1.16	-4.55
11(cement)	0.90	-5.90
20B(cement)	0.98	-7.13
23(cement)	-0.15	-6.83
81(cement)	0.27	-7.84
73B(cement)	0.23	-9.34
26(brachiopoda)	1.97	-3.94
30(brachiopoda)	1.64	-2.04
41(brachiopoda)	1.51	-3.99
45(brachiopoda)	1.42	-2.16
54(brachiopoda)	-0.11	-7.91
73A(brachiopoda)	2.51	-3.17
112(brachiopoda)	-2.40	-7.64
119(brachiopoda)	-0.08	-8.47
8B-A(brachiopoda)	1.86	-5.84

Table 2

Sample No.	Ca (wt%)	Mg (wt%)	Na (ppm)	Sr (ppm)	Fe (ppm)	Mn (ppm)	Sr/Na
13 (ooid)	36.45	0.94	8470	270	9070	850	0.03
20 (ooid)	36.22	0.50	10410	110	8000	810	0.10
49 (ooid)	37.47	0.34	8180	280	8930	720	0.03
5B (ooid)	37.55	0.33	18790	230	4840	880	0.10
6B (ooid)	36.59	0.42	10500	110	4360	810	0.03
97 (micrite)	36.57	0.35	6260	220	6440	530	0.03
99 (micrite)	37.80	0.33	6200	400	950	600	0.07
100 (micrite)	36.01	1.50	2600	300	4740	770	0.85
105 (micrite)	37.21	0.77	3260	310	5080	570	0.09
106 (micrite)	36.01	1.40	2950	180	6350	730	0.06
25B (micrite)	36.77	0.45	4710	290	5770	830	0.06
32 B (micrite)	36.24	0.41	1260	160	2620	1140	0.13
33 B (micrite)	36.12	0.53	3360	170	5660	1060	0.05
36 (micrite)	37.58	1.32	5030	130	7940	1070	0.03
43 B (micrite)	37.99	1.11	3020	130	6180	700	0.04
11 (cement)	39.13	0.88	3770	220	8090	590	0.08
1B (cement)	36.40	0.59	13010	230	7630	880	0.02
33 (cement)	37.50	0.60	1.326	410	8200	8700	0.74
49 (cement)	36.01	0.49	11380	270	7380	770	0.024
73 (cement)	38.19	0.36	2940	240	9890	610	0.08
81 (cement)	38.39	0.58	12140	240	5410	450	0.01
26 (brachiopod)	38.74	1.002	20000	340	8660	880	0.01
30 (brachiopod)	37.66	0.33	4290	450	7470	910	0.10
41 (brachiopod)	38.81	2.42	10170	140	8360	710	0.01
45 (brachiopod)	36.05	0.28	9250	400	6180	470	0.04
54 (brachiopod)	38.43	1.12	5970	320	8120	880	0.08
73 (brachiopod)	36.53	0.23	8770	450	5870	450	0.04
8B-A (brachiopod)	38.99	0.57	16760	290	4350	530	0.02
112 (brachiopod	38.45	0.94	4760	270	5660	600	0.06
119 (brachiopod)	36.19	0.54	5030	280	5000	350	0.07

Table 3